Characterization of flow units in metallic glass through density variation

R. J. Xue, D. P. Wang, Z. G. Zhu, D. W. Ding, B. Zhang et al.

Citation: J. Appl. Phys. **114**, 123514 (2013); doi: 10.1063/1.4823816
View online: http://dx.doi.org/10.1063/1.4823816
View Table of Contents: http://jap.aip.org/resource/1/JAPIAU/v114/i12
Published by the AIP Publishing LLC.

Characterization of flow units in metallic glass through density variation

R. J. Xue,[1] D. P. Wang,[2] Z. G. Zhu,[2] D. W. Ding,[2] B. Zhang,[1,a)] and W. H. Wang[2,a)]
[1]*School of Materials Science and Engineering, Hefei University of Technology, Hefei 230009, China*
[2]*Institute of Physics, Chinese Academy of Sciences, Beijing 100190, China*

(Received 19 August 2013; accepted 13 September 2013; published online 30 September 2013)

The evolution of flow units associated with the flow "defects" in metallic glass is characterized by monitoring the metallic glassy density change upon isothermal annealing far below their glass transition temperature. A meaningful function for the density variation with the concentration of flow units is obtained for the metallic glasses. We show that the correlation between the density variation and the flow unit have implications for understanding the fragility, structural heterogeneous, and structural relaxation behaviors in metallic glasses. © *2013 AIP Publishing LLC*. [http://dx.doi.org/10.1063/1.4823816]

I. INTRODUCTION

Intensive studies have proved that the metallic glasses (MGs) are actually intrinsic microstructural heterogeneous, and the heterogeneous MG can be regarded as liquid-like soft regions containing higher free volumes embedded in solid glassy substrate.[1–8] Experimental and simulation evidences demonstrate that the nano-scale liquid-like regions have higher energy and low elastic moduli compared to that of the substrate. Similar to the defects in crystalline solids, the liquid-like regions act as flow units during the deformation, relaxations, and glass transition in MGs.[4–12] That is, the flow units are the nano-scale liquid-like regions where the atoms are loosely packed and embedded in solid glassy substrate, and the atoms in a flow unit can cooperatively move under applied stress and/or temperature.[3–12] The flow unit model is useful for understanding the anelastic and plastic deformation behaviors and the structural origin of the β-relaxation in MGs.[9,12]

Previous investigations suggest that inhomogeneous microstructure may be due to the existence of flow units in MGs;[4,8] however, the definite relationship between microstructural and defects of flow units is not clear yet, and it is also difficult to identify and characterize the flow units in structural disordered glasses.[3,13–22] The density has been known as one of the most available physical parameter to monitor the structural evolution, which could be related to the flow units change of MGs in isothermal relaxation[16–18] When the as-cast MG is isothermally annealed at a given temperature below glass transition temperature T_g for various times, the density increases with the time towards an equilibrium value, which could reflect the evolution, annihilation, and concentration variation of defects of potential flow units in MGs.[19–21]

In this paper, we study and characterize the flow units in three typical MGs through monitoring their density values change upon isothermal annealing time below T_g. An equation is obtained for the interrelationship between the density and concentration of flow units in MGs. The flow unit model can explain the microstructural evolution and the kinetics of structural relaxation during isothermal annealing process in MGs. We also discuss the possible picture for the activation and evolution of flow units based on our observations.

II. EXPERIMENTS

We selected three MGs, $Zr_{52.5}Cu_{17.9}Ni_{14.6}Al_{10}Ti_5$ (vit105), $(Cu_{50}Zr_{50})_{92}Al_8$, and $Pd_{40}Ni_{10}Cu_{30}P_{20}$, that have good glass-forming ability, markedly different fragility, mechanical, chemical, and physical properties, and microstructural characteristics.[23–25] The vit105 and $(Cu_{50}Zr_{50})_{92}Al_8$ MGs were prepared by arc melting in a Ti-gettered argon atmosphere; the $Pd_{40}Ni_{10}Cu_{30}P_{20}$ MG was prepared by induction melting in a high-vacuum quartz tube. The alloy ingots were remelted and sucked into a Cu mold to obtain cylindrical rods with 5 mm diameter, respectively. The structures of the as-cast alloys were ascertained using X-ray diffraction (XRD) in a MAC M03 XHF diffractometer with Cu Kα radiation. Thermal analysis was carried out using different scanning calorimetry (DSC; Perkin-Elmer DSC8000) at a heating rate of 20 K·min^{-1}. The density ρ was measured by Archimedean technique, and the samples of the MGs make the density measurements (the sample weights larger than 1.0 g) to have higher accuracy (within 0.1%). The $Pd_{40}Ni_{10}Cu_{30}P_{20}$ and $(Cu_{50}Zr_{50})_{92}Al_8$ samples were isothermally annealed at $0.88T_g$ for various times in a furnace under a vacuum of $\sim 2 \times 10^{-3}$ Pa; the vit105 sample was annealed in a furnace under a vacuum of $\sim 1 \times 10^{-5}$ Pa and cooled down to room temperature to measure density, DSC, and XRD. We chose the annealing temperature of $0.88T_g$ because it is the optimal annealing temperature for avoiding crystallization and decrease the annealing time to reach the density saturation.[25]

III. RESULTS AND DISCUSSION

Figure 1(a) shows XRD patterns of the $Pd_{40}Ni_{10}Cu_{30}P_{20}$, vit105, and $(Cu_{50}Zr_{50})_{92}Al_8$ MGs in as-cast and annealed (at $0.88T_g$ for 259, 256, and 260 h, respectively) states. The as-quenched MGs have the typical amorphous characteristic. Figure 1(b) gives three continuous DSC traces for as-quenched $Pd_{40}Ni_{10}Cu_{30}P_{20}$, vit105, and $(Cu_{50}Zr_{50})_{92}Al_8$

a)Authors to whom correspondence should be addressed. Electronic addresses: bo.zhang@hfut.edu.cn and whw@iphy.ac.cn

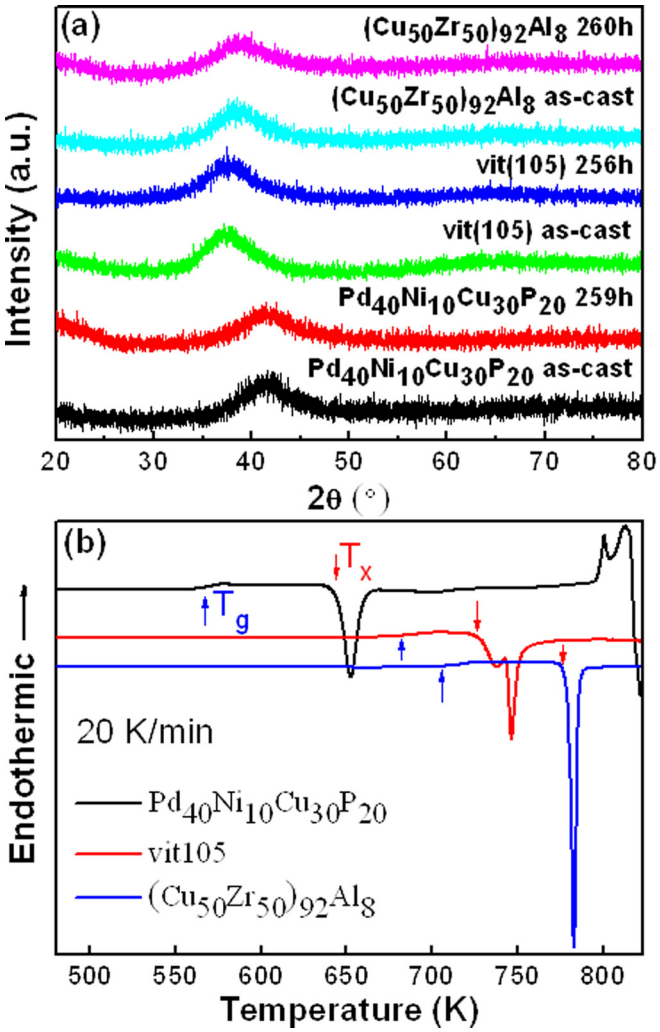

FIG. 1. (a) XRD patterns of $Pd_{40}Ni_{10}Cu_{30}P_{20}$, vit105, and $(Cu_{50}Zr_{50})_{92}Al_8$ MGs in as-quenched and annealed (for 259, 256, and 260 h, respectively); (b) DSC traces focusing on glass transition and crystalline process of the three MGs.

MGs. The distinct glass transition and sharp crystallization peaks confirm the glassy structure of the three alloys. The wide supercooled liquid regions indicate that the three MGs have high thermal stability. The detailed thermodynamic parameters, such as T_g and supercooled liquid region ΔT_x, of the three MGs are summarized in Table I. In order to avoid the influence of the effects of crystallization, we annealed the three MGs at their $0.88T_g$ ($0.88T_g$ of $Pd_{40}Ni_{10}Cu_{30}P_{20}$, vit105, and $(Cu_{50}Zr_{50})_{92}Al_8$ at 496, 600, 619 K, separately). The XRD patterns in Fig. 1(a) show that the annealed MGs have no significant difference compared to the as-cast samples, and no obvious crystalline peaks can be observed up to 260 h annealing within the examining limit of XRD. The results indicate that the three MGs indeed have high stability at $0.88T_g$. The positions of the typically diffused amorphous peaks shift to the higher angle, and the intensity of the scattering peaks decrease compared to that of the as-prepared MGs [see Fig. 1(a)]. This suggests that the microstructure change of these MGs is induced by the isothermally annealing, and the change is due to the annihilation of the "defects" of flow units.

Figure 2(a) presents density variation evolution behavior of $Pd_{40}Ni_{10}Cu_{30}P_{20}$, vit105, and $(Cu_{50}Zr_{50})_{92}Al_8$ MGs at $0.88T_g$. The relative density change $\Delta\rho = [\rho(t) - \rho(0)]/\rho(0)$ [where $\rho(0)$ and $\rho(t)$ are the density of the as-cast and annealed MGs for time t, respectively] increases rapidly with the annealing time in the initial 10 h. After 128 h annealing, the density shows minor changes and approaches a saturation value $\Delta\rho(\infty)$ $[\Delta\rho(\infty) = (\rho(\infty) - \rho(0))/\rho(0)]$. When $t \to \infty$, the density $\rho(\infty)$ approaches an equilibrium value of this annealing temperature, which can be regarded as the density of its corresponding perfect crystal. We note that one cannot reach $\rho(\infty)$ in experiment annealing time scale because it is longer than years.[26]

Based on hard sphere dense random packing model of MG,[27,28] the atom packing fraction φ (the volume occupied by atoms with known atomic radii in one molar volume) can be estimated from the molar volume $V_m = \frac{M}{\rho}$ as:[29] $\phi = \sum_i \frac{4}{3} n_i \pi {R_i}^3 / V_m$, where R_i is the atomic radius of element i, n_i is the number of atom i in one molar alloy, and M is molar mass. Figure 2(b) shows the change tendency of the φ of $Pd_{40}Ni_{10}Cu_{30}P_{20}$ MG with annealing time, and one can see that the φ has the same change trend with that of density. That means the isothermal annealing induces efficient denser atoms packing, and the MGs have a higher packing fraction after the annealing.[30] Because a MG consists of solid phase where the atoms are densely and randomly packed and liquid-like flow units where the atoms packed relatively loose, the increase of density or φ with annealing time can be attributed to the annihilation of some flow units with lower activation energy and shrinking of the larger flow units.

We try to fit the density evolution upon annealing and find that the density changes during the isothermal annealing process of the MGs with markedly different glass-forming ability, properties, and microstructural characteristics can be best fitted by

TABLE I. The thermodynamic parameters T_g, ΔT_x ($\Delta T_x = T_x - T_g$, T_x is crystallization temperature), initial density value $\rho(0)$, equilibrium density value $\rho(\infty)$, relative density change saturation value $\Delta\rho(\infty)$, fragility m, and activation energy of flow units W of $Pd_{40}Ni_{10}Cu_{30}P_{20}$, vit105, and $(Cu_{50}Zr_{50})_{92}Al_8$ MGs, and fitting parameters A, B, and β for their density evolution curves at $0.88T_g$. $\Delta c = c(0) - c(\infty) = c(0)$ correspond to the concentration of flow units in as-cast state of MGs.

Glass	T_g (K)	ΔT_x (K)	m	W (kJ/mol)	$\rho(0)$ (g/cm^3)	$\rho(\infty)$ (g/cm^3)	$\Delta\rho(\infty)$ (%)	Δc (%)	β	A	B
$Pd_{40}Ni_{10}Cu_{30}P_{20}$	563	83	58 (Ref. 34)	129 (Ref. 9)	9.173	9.256	0.905	0.895	0.103 ± 0.005	$8.62(\pm 0.05) \times 10^{-22}$	0.07 ± 0.01
Vit105	682	57	49 (Ref. 35)	147 (Ref. 40 and 41)	6.694	6.748	0.807	0.819	0.115 ± 0.006	$1.24(\pm 0.02) \times 10^{-19}$	0.17 ± 0.02
$(Cu_{50}Zr_{50})_{92}Al_8$	703	77	43 (Ref. 36)	174 (Ref. 9)	7.108	7.154	0.647	0.643	0.162 ± 0.008	$1.65(\pm 0.02) \times 10^{-14}$	0.56 ± 0.06

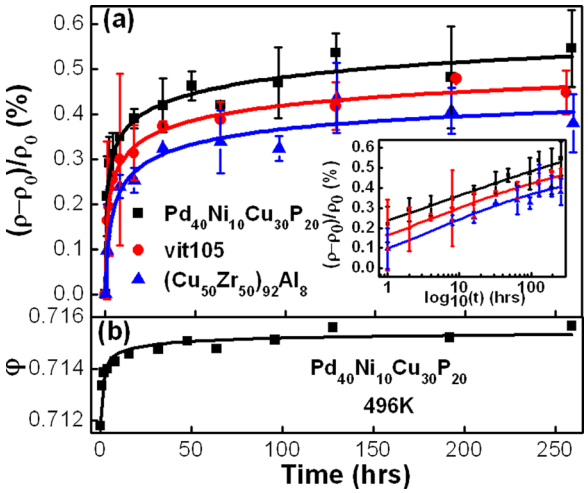

FIG. 2. (a) The relative variation of density $\Delta\rho$ (%) vs. t (h) of $Pd_{40}Ni_{10}Cu_{30}P_{20}$, vit105, and $(Cu_{50}Zr_{50})_{92}Al_8$ MGs at $0.88T_g$ that $\Delta\rho = [\rho(t) - \rho(0)]/\rho(0)$, density ρ evolution upon annealing can be best fitted by $\rho(t) = \frac{\rho(\infty)}{1+c}$, the inset shows the logarithmic annealing time scale vs. the relative variation of density $\Delta\rho(\%)$. (b) The atom packing fraction vs. annealing time t (h) of $Pd_{40}Ni_{10}Cu_{30}P_{20}$ MG at 496 K.

$$\rho(t) = \frac{\rho(\infty)}{1+c}, \tag{1}$$

where $c = \left(\frac{A}{B+t}\right)^{\beta}$, A, B, and exponent β are the fitting parameters, which relate the component of MG and annealing temperature. The fitting values of A, B, and β are listed in Table I. When $t \to \infty$ and $c(\infty) \to 0$, ρ approaches the density value $\rho(\infty)$ of its corresponding crystal; when $t = 0$, $c = (A/B)^{\beta}$ corresponds to concentration of flow units in as-quenched state of MG. The value of exponent β is less than unity and reflects the sensitivity of the flow unit concentration change upon t. Therefore, the c reflects the trends of microstructural attenuation with the increasing annealing time and correlates with the concentration of flow units. Therefore, Eq. (1) gives the relationship between the density and concentration of flow units in MGs. On the other hand, for a given annealing temperature, the change of the concentration of flow units c of a MG upon annealing time t can be determined by density as

$$c(t) = [\rho(\infty) - \rho(t)]/\rho(t). \tag{2}$$

Next, we show that the interrelationship between the density and concentration of flow units of Eq. (1) is useful for understanding of the structural inhomogeneous, fragility, flow units activation, and structural characteristic of MGs. As shown in Table I, the three MGs with similar density change tendency (corresponding to the change tendency of the concentration of flow units) upon annealing time have different fitting parameters, and the difference indicates that the concentration of flow units of a MG could determine its fragility, structural characteristics, and flow unit activation. The fragility (m) characterizes the degree of strength or fragileness of glass-forming liquid and reflects the structural heterogeneity of a MG,[31–33] and the smaller value of fragility indicates that the structure of a liquid less sensitive to the temperature changes and becomes more stable.[31,33] The m of $Pd_{40}Ni_{10}Cu_{30}P_{20}$ MG is 58,[34] vit105 MG is 49,[35] and $(Cu_{50}Zr_{50})_{92}Al_8$ MG is 43,[36] which ranges from fragile to strong. The saturation values $\Delta\rho(\infty)$ of $Pd_{40}Ni_{10}Cu_{30}P_{20}$ (0.905%), vit105 (0.807%), and $(Cu_{50}Zr_{50})_{92}Al_8$ (0.647%) (see Table I) range from large to small and match the difference of m for the three MGs. The Δc $[= c(0) - c(\infty) = c(0)]$ of $Pd_{40}Ni_{10}Cu_{30}P_{20}$, vit105, and $(Cu_{50}Zr_{50})_{92}Al_8$ MGs, which corresponds to the concentration of flow unit in as-cast state, are 0.895%, 0.819%, and 0.643%, respectively. The comparison of m, $\Delta\rho(\infty)$, and Δc of the three MGs demonstrates that strong glass possesses a relatively low concentration of the flow units, lower density change upon annealing, the small saturation value of relative density $\Delta\rho(\infty)$, and relatively homogeneous microstructure; and the fragile MG has larger concentration of flow units, larger density change upon annealing, and more inhomogeneous structure, which are in agreement with the previous predictions.[13,37] The results indicate that the change of concentration of flow unit and the saturation value $\Delta\rho(\infty)$ can reflect the structural heterogeneity of a MG.

The flow unit volume can be expressed as:[38] $\Omega = nC_fV$, where n is the number of atoms in a flow unit and the constant $C_f \approx 1.1$. V is the average atomic volume expressed as $V = M/(\rho N_A)$, where N_A is the Avogadro constant. The n of $Pd_{40}Ni_{10}Cu_{30}P_{20}$, $(Cu_{50}Zr_{50})_{92}Al_8$, and vit105 is about 241, 251,[9] and 215,[9,38,39] respectively. Figure 3 exhibits average volume Ω change of $Pd_{40}Ni_{10}Cu_{30}P_{20}$, vit105, and $(Cu_{50}Zr_{50})_{92}Al_8$ MGs with annealing time t at 496, 600, and 619 K, respectively. The Ω decreases with t, indicating that the flow units of MG become smaller even annihilate with isothermal annealing. The results provide information about the evolution of a flow unit during isothermal annealing process as schematically illustrated in Fig. 4. The pink and violet atoms represent the defects of flow unit in MGs with higher potential energies and the looser packing densities compared with the relatively homogeneous matrix denoted by the blue atoms. The atoms in flow unit are the preferred sites for the relaxation caused by annealing, and the rearrangement of atoms initiates preferably in these active zones and causes the atoms to relax to lower energy state, which is schematically illustrated by the disappearance of the

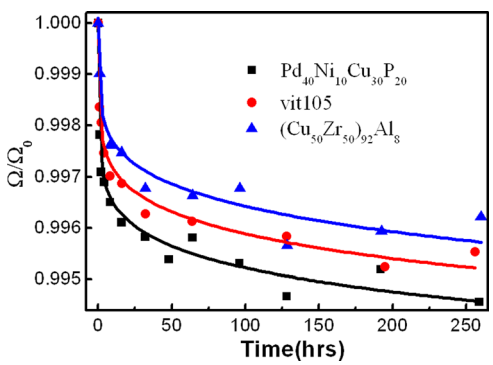

FIG. 3. The normalized volume of a flow unit Ω/Ω_0 [Ω_0 and Ω are the volume of a flow unit of the quenched and annealed MG for time t, respectively] vs. annealing time t (h) of $Pd_{40}Ni_{10}Cu_{30}P_{20}$, vit105, and $(Cu_{50}Zr_{50})_{92}Al_8$ MGs at 496, 600, 619 K, separately.

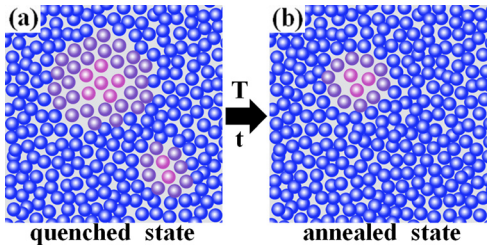

FIG. 4. Schematic illustrations of evolution of flow units of MGs during annealing. (a) Before annealing, the violet and pink atoms areas represent the defects of low unit in MGs with higher potential energies and looser packing densities compared with the relatively homogeneous and denser packed matrix denoted by the blue atoms. (b) The shrinking of the volume and annihilation of the flow units during annealing process.

higher-energy pink atoms and the spread of violet or blue atom areas. Meanwhile, the volumes of some flow units are shrunk as the annealing time increases. Hence, the annealing actually leads to an evolution process of flow units from size decrease to annihilation in MG. The flow unit variations are reversed in loading case, and with the increase of loading stress, the volume of the flow unit expands, which is the activation process of the flow units.[22]

The average activation energy of flow units W can be estimated according to $W \approx 26RT_g$.[9,40,41] The W of $Pd_{40}Ni_{10}Cu_{30}P_{20}$, vit105, and $(Cu_{50}Zr_{50})_{92}Al_8$ is 129 kJ mol^{-1},[9] 147 kJ mol^{-1},[40,41] and 174 kJ mol^{-1},[9] respectively. As shown in Figs. 2 and 3, the ascending of the density and descending of volume of the flow unit of Pd-based MG is faster than that of vit105 and CuZr-based MG with the annealing time. This is due to the low activation energy or faster relaxation of the flow units in Pd-based MG, which indicates that the evolution of the flow units in MG with low activation energy is much faster and easier than that in vit105 and CuZr-based MGs, which is consistent with recent nanoindentation experimental results.[42] From Table I, one can also see that the MG with smaller average flow unit activation energy of W has larger density variation $\Delta\rho$, which indicates that the "defects" of flow units in the MG with lower W can be readily annihilated.

IV. CONCLUSIONS

We obtain the interrelationship between the density variation and concentration of flow units in metallic glasses through monitoring density variation during the isothermal annealing processes. A function for the density variation with the concentration of flow units is obtained for the metallic glasses. The correlation can be applied to understand the fragility, structural heterogeneous, flow units evolution process, and microstructural characteristics of MGs.

ACKNOWLEDGMENTS

The experimental assistance and insightful discussion with D. Q. Zhao, H. Y. Bai, and P. Wen are appreciated. This work was supported by the NSF of China (51171055 and 51271195).

[1]P. G. Debenedetti and F. H. Stillinger, Nature **410**, 259 (2001).
[2]T. Egami, S. J. Poon, Z. Zhang, and V. Keppens, Phys. Rev. B **76**, 024203 (2007).
[3]W. Dmowski, T. Iwashita, C. P. Chuang, J. Almer, and T. Egami, Phys. Rev. Lett. **105**, 205502 (2010).
[4]H. Wagner, D. Bedorf, S. Kuchemann, M. Schwabe, B. Zhang, W. Arnold, and K. Samwer, Nature Mater. **10**, 439 (2011).
[5]H. B. Yu, Z. Wang, W. H. Wang, and H. Y. Bai, Phys. Rev. Lett. **108**, 015504 (2012).
[6]Y. H. Liu, D. Wang, K. Nakajima, W. Zhang, A. Hirata, T. Nishi, A. Inoue, and M. W. Chen, Phys. Rev. Lett. **106**, 125504 (2011).
[7]W. Jiao, P. Wen, H. L. Peng, H. Y. Bai, B. A. Sun, and W. H. Wang, Appl. Phys. Lett. **102**, 101903 (2013).
[8]J. C. Ye, J. Lu, C. T. Liu, Q. Wang, and Y. Yang, Nature Mater. **9**, 619 (2010).
[9]S. T. Liu, Z. Wang, H. L. Peng, H. B. Yu, and W. H. Wang, Scr. Mater. **67**, 9 (2012).
[10]S. T. Liu, W. Jiao, B. A. Sun, and W. H. Wang, J. Non-Cryst. Solids **376**, 76 (2013).
[11]Y. Yang, J. F. Zeng, J. C. Ye, and J. Lu, Appl. Phys. Lett. **97**, 261905 (2010).
[12]Z. Wang, P. Wen, L. S. Huo, H. Y. Bai, and W. H. Wang, Appl. Phys. Lett. **101**, 121906 (2012).
[13]R. Busch, E. Bakke, and W. L. Johnson, Acta Mater. **46**, 4725 (1998).
[14]I. Gallino, M. B. Shah, and R. Busch, Acta Mater. **55**, 1367 (2007).
[15]S. V. Khonik, A. V. Granato, D. M. Joncich, A. Pompe, and V. A. Khonik, Phys. Rev. Lett. **100**, 065501 (2008).
[16]O. Haruyama and A. Inoue, Appl. Phys. Lett. **88**, 131906 (2006).
[17]W. H. Wang, R. J. Wang, W. T. Yang, B. C. Wei, P. Wen, D. Q. Zhao, and M. X. Pan, J. Mater. Res. **17**, 1385 (2002).
[18]H. S. Chen, J. Appl. Phys. **49**(6), 3289 (1978).
[19]F. Spaepen, Acta Metall. **25**, 407 (1977).
[20]M. H. Cohen and D. Turnbull, J. Chem. Phys. **31**, 1164 (1959).
[21]A. J. Kovacs, R. A. Stratton, and J. D. Ferry, J. Phys. Chem. **67**, 152 (1963).
[22]L. S. Huo, J. Ma, H. B. Ke, H. Y. Bai, D. Q. Zhao, and W. H. Wang, J Appl. Phys. **111**, 113522 (2012).
[23]W. H. Wang, Prog. Mater. Sci. **57**, 487 (2012).
[24]W. H. Wang, J. J. Lewandowski, and A. L. Greer, J. Mater. Res. **20**, 2307 (2005).
[25]Z. G. Zhu, P. Wen, D. P. Wang, R. J. Xue, D. Q. Zhao, and W. H. Wang, J. Appl. Phys. **114**, 083512 (2013).
[26]S. F. Swallen, K. L. Kearns, M. K. Mapes, Y. S. Kim, R. J. McMahon, M. D. Ediger, T. Wu, L. Yu, and S. Satija, Science **315**, 353 (2007).
[27]J. D. Bernal, Nature **185**, 68 (1960).
[28]T. Egami and Y. Waseda, J. Non-Cryst. Solids **64**, 113 (1984).
[29]A. Meyer, Phys. Rev. B **66**, 134205 (2002).
[30]D. B. Miracle, Acta Mater. **61**, 3157 (2013).
[31]C. A. Angell, Science **267**, 1924 (1995).
[32]B. Zhang, R. J. Wang, D. Q. Zhao, M. X. Pan, and W. H. Wang, Phys. Rev. B **73**, 092201 (2006).
[33]C. A. Angell, J. Non-Cryst. Solids **73**, 1 (1985).
[34]J. F. Löffler, J. Schroers, and W. L. Johnson, Appl. Phys. Lett. **77**, 681 (2000).
[35]Z. Evenson, T. Schmitt, M. Nicola, I. Gallino, and R. Busch, AIP Conf. Proc. **1518**, 197 (2012).
[36]P. Yu, H. Y. Bai, and W. H. Wang, J. Mater. Res. **21**, 1674 (2006).
[37]H. Tanaka, Phys. Rev. Lett. **90**, 055701 (2003).
[38]M. L. Falk and J. S. Langer, Phys. Rev. E **57**, 7192 (1998).
[39]W. L. Johnson and K. Samwer, Phys. Rev. Lett. **95**, 195501 (2005).
[40]J. Perez and J. Y. Cavaille′, J. Non-Cryst. Solids **172**, 1028 (1994).
[41]H. B. Yu, W. H. Wang, H. Y. Bai, Y. Wu, and M. W. Chen, Phys. Rev. B **81**, 220201(R) (2010).
[42]X. L. Bian, G. Wang, K. C. Chan, J. L. Ren, Y. L. Gao, and Q. J. Zhai, Appl. Phys. Lett. **103**, 101907 (2013).